Journal Pre-proof

Cenozoic exhumation history at the core of the Andes at 31.5°S revealed by apatite fission track thermochronology

Ana Lossada, Julieta Suriano, Laura Giambiagi, Paul G. Fitzgerald, Greg Hoke, José Mescua, Ana Tedesco, Guadalupe Arzadún, Sofía Bordese

PII: S0895-9811(20)30294-7

DOI: https://doi.org/10.1016/j.jsames.2020.102751

Reference: SAMES 102751

To appear in: *Journal of South American Earth Sciences*

Received Date: 18 February 2020

Revised Date: 29 June 2020

Accepted Date: 10 July 2020

Please cite this article as: Lossada, A., Suriano, J., Giambiagi, L., Fitzgerald, P.G., Hoke, G., Mescua, José., Tedesco, A., Arzadún, G., Bordese, Sofí., Cenozoic exhumation history at the core of the Andes at 31.5°S revealed by apatite fission track thermochronology, *Journal of South American Earth Sciences* (2020), doi: https://doi.org/10.1016/j.jsames.2020.102751.

Suriano: methodology, conceptualization

Giambiagi: methodology, conceptualization

Fitzgerald: methodology, software, Writing – Review & Editing

Hoke: conceptualization, software, Writing – Review & Editing

Mescua: conceptualization, Writing – Original Draft

Tedesco: methodology

Arzadún: methodology

Bordese: methodology

Cenozoic exhumation history at the core of the Andes at 31.5°S revealed by apatite fission track thermochronology

Ana Lossada[1*], Julieta Suriano[2], Laura Giambiagi[2], Paul G. Fitzgerald[3], Greg Hoke[3], José Mescua[2, 4], Ana Tedesco[5], Guadalupe Arzadún[6], Sofía Bordese[6]

1: IDEAN, CONICET, Buenos Aires, Argentina

2: IANIGLA, CCT-MENDOZA, CONICET, Mendoza, Argentina

3: Department of Earth Sciences, Syracuse University, Syracuse, NY, EEUU

4: FCEN, UNCUYO, Mendoza, Argentina

5: SEGEMAR, Argentina

6: LA.TE ANDES S.A., Salta, Argentina

*corresponding author (ana.c.lossada@gmail.com)
Intendente Güiraldes 2160
Ciudad Universitaria - Pabellón II
C1428EGA – CABA, Argentina

Abstract

The Andes at ~31°-32°S lie above the Chilean-Pampea n flat slab zone (~27-33°S), where several morphostructural units developed resulting in a large orogenic width. The core of the Andes is composed of the La Ramada fold-and-thrust belt in Principal Cordillera and the basement blocks of Frontal Cordillera. While rock uplift of these blocks has been broadly constrained to the middle Miocene based on structural and provenance studies, thermochronologic approaches with the potential to directly constrain the timing and amount of exhumation have not been exploited until recently. Apatite fission track data from a ~1 km vertical profile collected within the Carboniferous Pico Los Sapos Batholith in the High Andes at 31.5°S places some constraints on the thermal evolu tion of the region since the Paleocene. The age-elevation profile combined with inverse thermal modeling and previous AHe thermochronology, indicates an episodic cooling/exhumation history. Rocks cooled rapidly in the early Cenozoic (ca. 65-55 Ma), followed by a period of relative thermal and tectonic stability when residence in an apatite partial annealing zone (PAZ) from at least ~52 Ma to ca.15 Ma, followed by final rapid cooling beginning ca. 15 Ma. We interpret early Cenozoic and middle Miocene rapid cooling events as to be related to erosional exhumation during Andean contractional phases, associated with thrust activity along the Mondaquita Fault. The age-elevation profile is partially duplicated, with upper samples being offset ~500 m due to back-thrusting since the late Miocene. The preservation of part of an exhumed PAZ indicates 3 to 5 km of exhumation since the onset of rapid cooling/exhumation at ~15 Ma. Although evidence for an early Cenozoic compressional phase in the High Andes at this latitude is scarce, the occurrence of a regional K-T (~65 Ma) unconformity supports our results. The Eocene Inca phase, registered north of 30°S, on the other hand, is not shown in our thermochronological data, suggesting that this tectonic phase did not affect the core of the Andes south of this latitude. Independent geological evidence both from the hinterland (structural, geochemical and thermochronological analyses) and foreland (provenance studies) corroborate our findings of a middle Miocene deformational event in the core of the Andes at 31.5°S.

Keywords Andes orogen, apatite fission-track thermochronology, Cenozoic exhumational history

1. Introduction

Low-temperature thermochronology can be used to resolve a wide range of tectonic and/or structural problems. In particular, apatite fission track (AFT) thermochronology provides constraints on the thermal (and hence exhumation) history of the uppermost crust (<5 km) (e.g., Gallagher et al., 1998; Reiners et al., 2006). The vertical profile approach uses samples collected over significant relief and a short horizontal distance (e.g., Fitzgerald et al., 1995; Braun, 2002; Huntington et al., 2007; Fitzgerald and Malusa, 2019). Typically, the vertical profile approach provides a more robust data interpretation than a series of isolated individual samples, although different sampling strategies are used to address different questions.

The Andes of Argentina and Chile represent the largest non-collisional orogen in the world, a result of a long-lived active oceanic-continent subduction, since at least the Jurassic (Mpodozis and Ramos, 1989; Oliveros et al., 2007). At ~31°-32°S, the Andes develop above the "Pampean" flat slab subduction segment (Fig. 1). Five morphostructural units subdivide the mountain chain, from west to east: the Coastal Range, Principal Cordillera, Frontal Cordillera, Precordillera and Pampean Ranges. At these latitudes, the timing of Cenozoic deformation was mainly constrained by unroofing analyses of the synorogenic deposits (Jordan et al. 1996; Perez, 2001; Pinto et al. 2018; Alarcon and Pinto, 2015; Levina et al., 2014), or structural relationships between units of known age (Ramos et al., 1996; Cristallini and Ramos, 2000; Perez, 2001; Mpodozis et al., 2009; Mpodozis, 2016, among others), and to a lesser degree by thermochronological studies (Levina et al., 2014; Rodriguez et al., 2018; Ortiz et al., 2015; Maydagán et al., 2020; Mahoney et al., 2019). However, at the core of the Andes, low temperature thermochronology has not been exploited until recently (Rodriguez et al., 2018; Maydagán et al., 2020). The uplift/deformation sequence of the different morphostructural units during the Cenozoic has been interpreted to be a result of a foreland advance of deformation related to the increase in the mechanical coupling between the Nazca and South American plates during the flattening of the slab (Jordan et al., 1983; Ramos et al., 2002; Ramos and Folguera, 2009; Martinod et al., 2013), since the middle Miocene. However, recent work performed in other sectors of the Southern Central Andes point toward significant exhumation/uplift in the Frontal Cordillera (Lossada et al., 2017, 2020; Riesner et al., 2019) and Precordillera (Levina et al., 2014; Suriano et al., 2017; Buelow et al., 2018) prior to the establishment of flat-slab conditions.

We apply AFT thermochronology in samples from a vertical transect collected at the core of the Andes at ~31.5°S with the objective to constrai n the cooling history and hene the timing of rock uplift-induced exhumation. With these results, we discuss if slab flattening may have cause the uplift and exhumation of the inner sector of the Andes.

2. Tectonic Setting

Above the Chilean-Pampean flat slab zone (~27-33°S, Jordan et al., 1983; Cahill and Isacks, 1992; Ramos et al, 2002; Kay and Mpodozis, 2002; Gans et al, 2011; Marot et al, 2014), the Andes are characterized by high mean elevations in the Principal and Frontal Cordilleras with the highest non-volcanic peaks in the Andes (Cerro Mercedario and Cerro Aconcagua peaks of > 6700 m a.s.l.), a lack of active arc-related magmatism, and a large orogenic width with basement-involved deformation resulting in the Pampean Ranges rising through the foreland (Jordan et al., 1983; Ramos et al., 2002). The large orogenic width is related to the influence of slab flattening since the Miocene because of greater coupling with the overriding South American plate.

In the westernmost sector, the Coastal Range consists of a metamorphic core interpreted as a late Paleozoic accretionary prism covered by Triassic to Cretaceous sedimentary and volcanic sequences (Rivano and Sepúlveda, 1991).

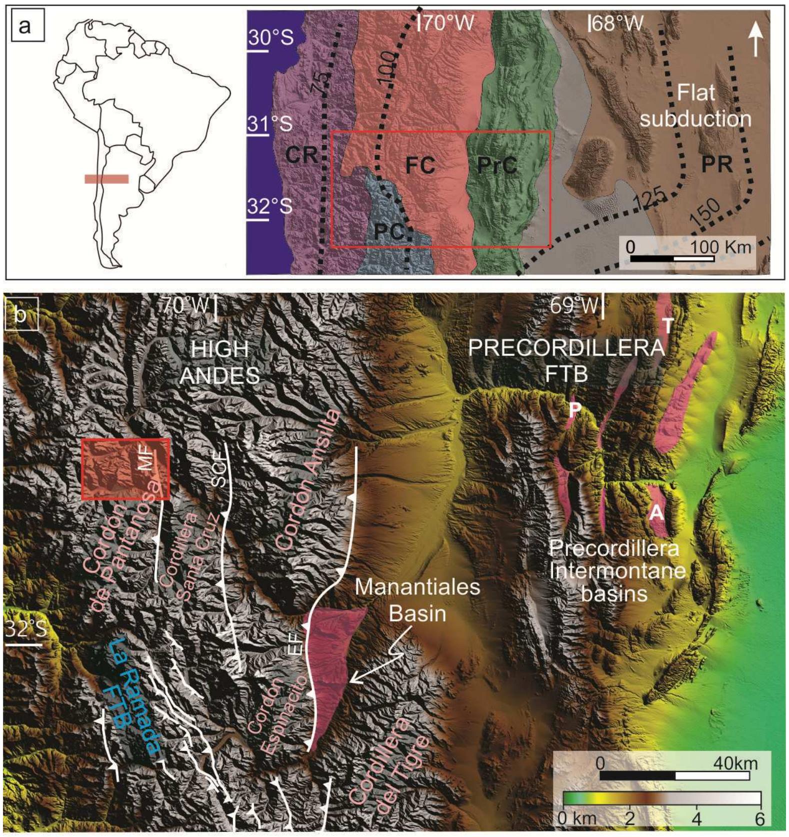

Figure 1: a) Location of the study area in the Pampean flat slab segment. The dashed black lines indicate contours of the Wadatti-Benioff zone (Cahill and Isacks, 1992). Morphostructural units: CR: Coastal Range, FC: Frontal Cordillera, PC: Principal Cordillera, PrC: Precordillera and PR: Pampean Ranges. b) Tectonic setting of the study zone (red rectangle) and location of Neogene synorogenic sedimentation (Manantiales Basin and Precordillera intermountain basins). In the High Andes, Frontal Cordillera ranges are in light pink letters and Principal Cordillera ranges in blue. MF: Mondaquita fault, SCF: Santa Cruz fault, EF: Espinacito fault, P: Pachaco, T: Talacasto, and A: Albarracín locations.

The High Andes at ~31°-32°S (Fig. 1) correspond to the northern extension of the Principal Cordillera and the Frontal Cordillera. The Principal Cordillera consists of a thick sequence of Mesozoic sedimentary rocks representing the northern end of the Neuquén Basin that are highly deformed into the La Ramada hybrid thin- and thick-skin fold-and-thrust belt during the early to middle Miocene (~20-18 Ma, Cristallini et al., 1994; Mpodozis and Ramos, 1989; Ramos et al., 1996, 2002; Alvarez and Ramos, 1999; Mpodozis et al., 2009). The Mesozoic sequences are intruded by Neogene plutons and covered by Neogene volcanic and volcaniclastic deposits (Mpodozis et al., 2009). The Frontal Cordillera comprises four N-trending basement-involved ranges where Carboniferous to Permian granitoids and Permo-Triassic Choiyoi Group volcanic rocks crop out (Mpodozis and Kay, 1990; Llambías and Sato, 1990; Sato and Llambías, 1993; Sato et al., 2015; Heredia et al. 2002). These ranges are, from west to east, the Cordón de Pantanosa, Cordillera de Santa Cruz, Cordón de Ansilta/Cordón del Espinacito and Cordillera del Tigre (Fig. 1b), uplifted by east-vergent thick-skin structures such as Mondaquita, Santa Cruz and Ansilta faults. Rock uplift of these blocks has been broadly constrained to the middle Miocene based on structural and provenance studies (Cristallini and Ramos, 2000; Pérez, 2001). Within the upper Paleozoic granitoids that crop out in the core of the mountain (Fig. 2), in the Cordón de Pantanosa range, we sampled the Pico Los Sapos Batholith (Mpodozis et al., 1976) comprising granodiorites and hornblende-biotite tonalites with upper Carboniferous to early Permian crystallization ages (Musso et al., 2012, Maydagán, 2012; Mpodozis, 2016).

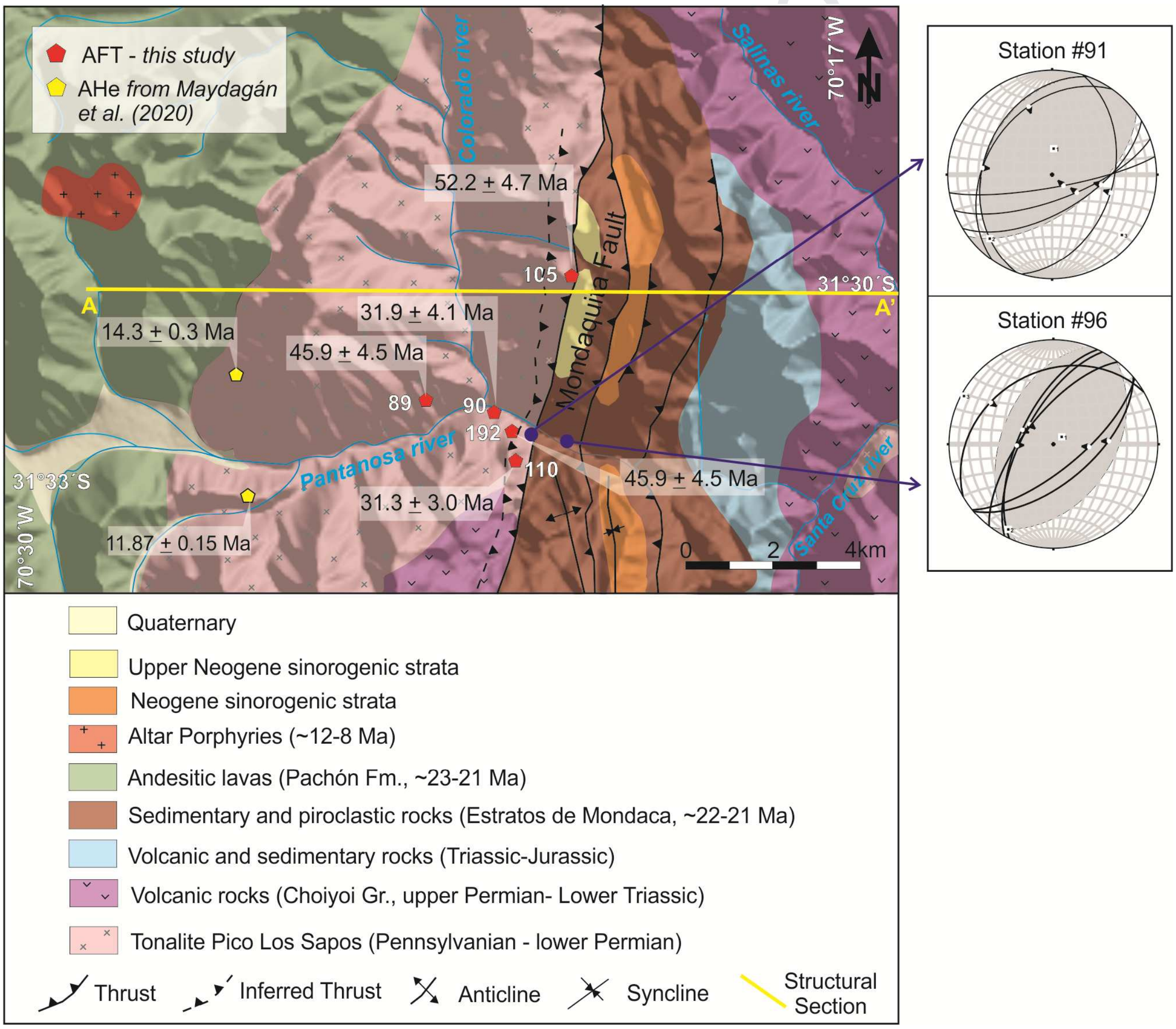

Figure 2: Simplified geologic map of the study area (modified from Bergoing Rubliar, 2016; Mpodozis, 2016; Maydagán et al. 2020), showing sampling site and location of AHe samples from Maydagán et al., (2020). Pachón

Fm. ages after Mpodozis et al. (2009) and Perelló et al. (2012). Estratos de Mondaca Fm. ages after Mpodozis et al. (2009). Altar Subvolcanic porphyritic intrusion ages after Maydagán et al. (2011, 2014). Blue dots indicate structural stations were inverse fault were measured. Kinematic axes have been computed using FaultKin (Allmendinger, 2001). Cross-section A-A' shown in Figure 5.

The Precordillera represents a fold-and-thrust belt developed on a Paleozoic passive margin sequence (Allmendinger et al., 1990; Allmendinger and Judge, 2014) since the middle Miocene (Levina et al., 2014).The Pampean Ranges consists of uplifted Proterozoic to lower Paleozoic magmatic-metamorphic basement blocks exhumed during the late Miocene to Pliocene, as a broken foreland progression of deformation related to the flattening of the slab (Ramos et al., 2002; Lobens et al., 2003).

Mpodozis et al. (2009) proposed a Neogene tectonic evolution for the different deformational domains in the High Andes at 31°-32°S based on geol ogical mapping, U-Pb dating and reinterpretation of the volcanic stratigraphy. These authors suggested that strong deformation in the Principal Cordillera occurred between ~22 and 17 Ma, based on U/Pb ages from syn- and post-tectonic granitoids, in agreement with U-Pb ages from Jara and Charrier (2004) suggesting two deformation events, one between 21 and 18 Ma, with the other after 18 Ma. Mpodozis et al. (2009) constrained fault activity in Frontal Cordillera south of our study area to <14 Ma, given that the Mondaquita Fault thrusts the Pachón Fm. (23-21 Ma, Mpodozis et al., 2009; Perelló et al., 2012, Fig. 2) over the middle Miocene volcanic rocks of Laguna del Pelado Volcanic Complex (18 Ma, Mpodozis et al., 2009) and the El Yunque Volcanic Unit (14 Ma, Mpodizis and Carnejo, 2012).

The uplift and exhumation history of the High Andes is recorded in the synorogenic deposits preserved in the Manantiales Basin, nested between different blocks of Frontal Cordillera, and in the intermountain basins located between the thrust sheets of Precordillera (Fig. 1). The Manantiales Basin (~32°S, Mirré, 1966; Perez, 1995; Jordan et al., 1996) is a retroarc foreland basin developed in front of the east-vergent La Ramada fold-thrust system during the Miocene. The infill of the Manantiales Basin, the Chinches Fm. consist of three members: a basal succession of ~350 m (the Areniscas Chocolate unit), Las Hornillas volcanic breccia, and finally more than 3000 m of coarse clastic fluvial strata and intercalated lacustrine deposits of the upper member. The unroofing studies carried out in this basin by Pérez (1995, 2001) and Jordan et al. (1996) constrain the timing of uplift and erosion of the La Ramada fold-and-thrust belt (~20 Ma) and the Frontal Cordillera blocks (between ~15 to 9 Ma). Alarcón and Pinto (2015) and Pinto et al. (2018) performed a sediment geochemical provenance study based on sandstone petrography, whole-rock geochemistry (major and trace elements) and U/Pb dating of the Chinches Fm. Based on a Maximum Depositional Age (MDA), they suggest that subsidence in the Manantiales Basin began at ~22 Ma, with a predominant provenance from Principal Cordillera, and reported a marked change in provenance trends to a Frontal Cordillera source at ~19 Ma, substantially earlier than previously proposed (Pérez, 2001; Jordan et al., 1996). Recent geochronologic and thermochronologic analyses (Mahoney et al., 2019; Mackaman-Lofland et al., 2020) constrained the beginning of subsidence to early Miocene (~17 to 19 Ma). Apatite (U-Th)/He dating from Chinches Fm. reported also by Mahoney et al. (2019) suggests that the succession underwent rapid exhumation between 9-7 Ma, presumably in response to propagation of the La Ramada thrust system to the east inverting the basin. This partially coincides with the wider range proposed by Mackman-Lofland et al. (2020) based on low temperature thermochronology in Manantiales basin (between 5 and 15 Ma).

In the Precordillera at 31°S, Levina et al. (2014) developed a depositional model based on sediment provenance analysis and U/Pb dating in some intermountain basins located within the thrust sheets along the San Juan river (Fig. 1). Their findings constrain the onset of activity in Frontal Cordillera at this latitude between 21 and 17 Ma, with the main phase of shortening between 17 and 12 Ma, as indicated by the shift in the sedimentation facies to a more energetic regime, and the increase in proportion of Permo-Triassic zircons.

3. Methodology

3.1 Apatite fission track thermochronology

Fission track (FT) thermochronology is based on the retention of radiation damage (fission tracks) formed during the spontaneous fission of ^{238}U in uranium-bearing minerals (commonly apatite or zircon). The closure temperature, that is the temperature of the dated mineral when the system closes and daughter start to accumulate while rock is undergoing steady monotonic cooling (Dodson, 1973), is on the order of 110ºC (±10ºC) for the AFT system, although it depends on apatite composition and cooling rate (e.g., Gleadow and Duddy, 1981; Gleadow et al., 1986; Green et al., 1989). The partial annealing zone (PAZ, Gleadow and Fitzgerald, 1987) for apatite is from ~120-60°C (e.g., Reiners and Br andon, 2006). Determining the concentration of ^{238}U and density of spontaneous fission tracks allows the determination of FT ages that, together with the kinetic parameter of confined track lengths, may provide constraints on the thermal history of rocks as they traverse the upper 4-5 km of the crust.

AFT ages were obtained at LA.TE Andes S.A. The measurements were performed with a Zeiss® AXIO Imager Z2m binocular microscope and Software TrackWorks® Autoscan®. A minimum of 25 grains per sample were counted and the confined horizontal spontaneous track length distributions were determined by measuring as many confined tracks as possible, considering that in all samples a unique central age was obtained. The diameter of etched spontaneous fission tracks measured parallel to crystallographic c-axis (Dpar) obtained for each grain counted or each grain where confined track lengths were measured serves as a composition proxy. The ages were calculated by the external detector method (ζ value) (Hurford and Green, 1982, 1983; Wagner Van den Haute, 1992; Gleadow, 1981), and the data processing with TrackKey© Software (Dunkl, 2002).

3.2 Sampling

Our sampling strategy was aimed at collecting "in situ" samples for AFT analyses from granitoids within the core of the Andes at the Cordón de Pantanosa range, sampling across an area of short-wavelength topography with the greatest relief possible. The objective is to capture a whole or part of an exhumed PAZ that allows to place constraints on the timing, amount, and/or rate of vertical crustal movements (as explained in Fitzgerald et al., 1995, Huntington et al., 2007 and Malusa and Fitzgerald, 2019). Five samples were collected from a ~0.9 km vertical profile at the Pantanosa River, immediately west of Mondaquita Fault (Fig. 2). At each sampling locality, ~ 5 kg of rock were collected from the upper Paleozoic Pico Los Sapos Batholith. Our sampling increments complement existing thermochronological data from a previous study in the area (Maydagán et al., 2020). All samples yielded enough apatites grains for FT dating, although unfortunately the amount of confined tracks lengths present in those grains was low.

3.3 Age-elevation profile

An age-elevation profile where AFT age is plotted versus sample elevation (Fig. 3a) allows the evaluation of variations in the apparent exhumation rate and is an approach that has been applied since the very early days of fission track analyses (e.g., Wagner and Reimer, 1972). During a relatively stable thermo-tectonic period, a characteristic profile of AFT ages is formed in the crust with apparent fission track ages decreasing with increasing depth (Gleadow and Duddy, 1981; Gleadow et al., 1983) (Fig. 3a). Subsequent rapid cooling/denudation may exhume this profile largely intact where is identified as an "exhumed or fossil PAZ" (Gleadow and Fitzgerald, 1987). A typical fossil PAZ profile is bounded by a distinct pair of "slope breaks" (Figure 3a; Fitzgerald et al., 1995) that mark the upper and lower limits of the exhumed PAZ, i.e. the paleo-isotherms of ~110℃ and ~60℃, respective ly. The lower, convex-up break in slope approximates the onset of the last rapid cooling/exhumation event that exhumed and exposed the profile. The lower part of the profile, below this lower break in slope, is steep, reflecting rapid cooling of samples. Confined track length distributions from samples in this part of the profile also reflect rapid cooling, with long mean track lengths (>14 μm) and unimodal form, because most of these tracks formed since the last rapid exhumation event. In turn, confined track lengths distributions from samples above the lower break in slope and which resided in the PAZ for considerable time contain many shortened partially anneled tracks , as well as longer tracks formed since the onset of rapid exhumation, resulting in a bimodal distribution with a shorter mean track length (<14 μm) (Fig. 3a). The segment of the age-elevation profile above the upper break in slope represents an older rapid cooling/exhumation period, prior to the development of the PAZ, and thus also has a steep slope. An apatite fission track age-elevation profile will not necessarily record all pulses of rapid cooling/exhumation, the apparent slope of an exhumed PAZ will vary depending on the length of time over which it formed and/or the relative thermal and tectonic stability during when it formed, and the characteristic "breaks in slope" may be missed. In these cases, utilization of inverse thermal modeling, incorporating confined track length distributions (the kinetic parameter), may help define the different segments of the curve. Although dependent on the tectonics of a particular region, the chances of capturing an exhumed fossil-PAZ in a vertical profile sampling are greater if samples are collected over the maximum possible relief (Fitzgerald et al., 1995).

3.4 Thermal history modeling

Inverse thermal modeling was undertaken on individual samples in the vertical profile in order to better constrain their thermal history. Modeling was performed using the program HeFTy 1.9.1 (Ketcham, 2005) utilizing the annealing algorithm from Ketcham et al. (2007a). HeFTy uses the Monte Carlo approach to model multiple time-temperature (t-T) trajectories, the results of which are the compared to FT data with paths being considered as “good” and “acceptable” fits using merit values of 0.5 and 0.05, respectively. In the modeled paths, HeFTy generates new nodal points between constraint windows with the mode between nodal points being episodic monotonic-variable, allowing trajectories to have the most freedom incorporating heating and cooling (HeFTy user manual; e.g., Ketcham, 2005). Modeled t-T paths were run until the ending condition of 20,000 paths were reached. AFT ages, confined track lengths (the kinetic parameter) and their angle to c axis, and Dpar values (composition proxy) are used as inputs. We applied the c-axis correction to the track length measurements, i.e., the angle of the confined track with respect to the c-axis of the grain that accounts for anisotropic annealing of fission tracks (e.g., Ketcham et al., 2007b). A final temperature around 10℃ was used according with the present elevation of the samples. Models were constrained very simply, with one initial t-T window and one final lower temperature constraint window (as shown in Figure 4). Chosen initial t-T window (between 100° and 200℃ f rom 60 to 100 Ma) is based on a geological constraint that sampled Pico Los Sapos Batholith and other Late Paleozoic to Triassic rocks represent the structural basement of the region (Cristallini and Ramos, 2000), covered by a thick column (~1 km) of Permo-Triassic Choiyoi Gr., ~1.5 km upper Triassic to lower to Cretaceous sedimentary and volcanic successions of the northernmost extension of the Neuquén Basin (Alvarez, 1996), and then ~1 km upper Cretaceous lavas and clastic deposits (Perelló et al., 2012; Mackaman-Lofland et al., 2019). Within the Pico Los Sapos Batholith, the basal levels were sampled (Fig. 5, T0). The lower temperature constraint range was between 0-20℃ from 10 Ma to present.

3.5 Structural cross-section

We performed a structural mapping of the Pantanosa area based on fieldwork, collection of fault-slip kinematic data, and satellite image interpretation. A balanced cross-section (A-A´, Fig. 2) running parallel to the direction of maximum contraction (west to east), was constructed along the study area, using 2D area-balancing techniques with the program MOVE©. The section was constrained by surface geology. Fault-parallel flow and trishear algorithms were employed to best match the model with observed geological relationships. The structural section was restored to key geological times to reconstruct the kinematic and deformation history according to our proposed thermal evolution (Fig. 5). We performed several models with different sample depths, varying the amount of slip along the Mondaquita Fault and the eastwards Santa Cruz Fault, until we found a T0 model that replicates the unconformity between the lower Miocene lavas (Pachón Formation) and the basement. As discussed below, the variation of AFT ages with elevation is used to constrain late-stage back-thrusting associated with the Mondaquita Fault. The inferred back-thrust is located inside the Mondaquita Fault damage zone (see kinematic data on stations 91 and 96, in Fig. 2).

4. Results and interpretation

The analytical results for the Pico Los Sapos Batholith vertical transect are presented in Table 1. The crystallization age of the samples is Pennsylvanian to lower Permian (Fig. 2), and there are no younger magmatic units close to the sampling localities (<25 km). Thus, we rule out cooling after thermal reheating to explain the AFT age pattern and interpret it as indicative of episodic cooling associated with two periods of exhumation. Moreover, rocks from the Eocene magmatic arc are located west of our study area, in Chile.

Sample	Location Lat./Long.	Elev. (m)	N	RhoD ($x10^6$ cm^{-2}) (Nd)	Rho-S ($x10^5$ cm^{-2}) (Ns)	Rho-I ($x10^6$ cm^{-2}) (Ni)	Age disp. (%)	$P(\chi^2)$ (%)	Central Age ±1σ (Ma)	[U] (ppm)	Confined track (mean length ± S.E., (N); µm)	Dpar (mean ± S.D.; µm)
Hb_Th 01-18-90	31.535°S 70.365°W	2915	33	7.01 (5000)	1.65 (164)	6.54 (650)	0.24	17.96	**31.9 ± 4.1**	13.99	**14.6 (1)**	1.4 ± 0.1
Hb_Th 01-18-89	31.535°S 70.382°W	3000	35	7.11 (5000)	2.62 (453)	7.25 (1251)	0.03	71.87	**45.9 ± 4.5**	14.52	**13.4 ± 0.6 (8)**	1.4 ± 0.3
Hb_Th 01-18-192	31.540°S 70.361°W	3060	35	6.69 (5000)	3.24 (533)	8.52 (1402)	0.16	17	**45.6 ± 4.6**	19.18	**13.2 ± 1.2 (11)**	1.5 ± 0.1
Hb_Th 01-18-110	31.545°S 70.363°W	3275	29	6.8 (5000)	9.53 (571)	37.08 (2223)	0.09	19.66	**31.3 ± 3.0**	78.91	**12.7 ± 1.1 (9)**	1.4 ± 0.1
Hb_Th 01-18-105	31.503°S 70.348°W	3866	35	6.9 (5000)	7.13 (1082)	16.82 (2551)	0.03	53.96	**52.2 ± 4.7**	35.74	**13.5 ± 0.9 (18)**	1.4 ± 0.2

Table 1: AFT results for Pantanosa River vertical sample at the core of the Andes at ~31.5°S. N: number of counted grains. Rho-D and Nd are the standard track density and number of tracks measured in the dosimeter. Rho-S and Ns are the fossil track density and number of spontaneous tracks measured on internal mineral surfaces. Rho-I and Ni are the induced track density and number of induced tracks measured. Standard and induced track densities were measured on mica external detectors (geometry factor of 0.5). $P(\chi^2)$>5 indicates an homogeneous grain age distribution with one population of cooling ages. Zeta value: 358.07 ± 23.83.

4.1 Age-elevation profile

In the vertical profile, samples present Eocene to Oligocene AFT central ages ranging from 52 to 31 Ma (Table 1, Fig. 3). The low dispersion found in all samples indicates that only one population of cooling ages is present within the grain age distributions. A narrow range in DPar values, 1.4-1.5 μm, indicate that the composition of the grains does not control the dispersion of the data. Although in general AFT ages decrease with decreasing elevation, there is no clear trend in the age-elevation profile to fit all samples (Fig. 3b). However, when interpreted in the context of an "exhumed PAZ" (e.g., Fitzgerald et al., 1995) the pattern of ages is treated as a partial duplication of an exhumed PAZ due to fault offset (Fig. 3c). The uppermost two samples (Hb_Th 01_18_105 and Hb_Th 01_18_110) define the upper-middle part of an exhumed PAZ, with the lower three samples defining the middle part of an exhumed PAZ. These two parts of profile are assumed to have the same approximate slope of about ~15 m/my, interpreted not as an apparent exhumation rate, but largely the relict slope of a PAZ that formed in a time of relative tectonic and thermal stability. We discuss this in more detail below, notably that an exhumed PAZ, when preserved is usually bound by two periods of rapid cooling, and the age-elevation profile by itself does not constrain the timing of these periods. The vertical offset between the two parts of the profile is ~500 m (see Fitzgerald and Malusa, 2019). There is a slight geographic/structural separation between these two groups of samples. In this case, the lower three samples are "down-dropped" with respect to the upper two samples, or vice-versa; that is, the upper two samples are up-thrust on an east-dipping thrust with respect to the lower two samples. This interpretation is supported by field observations that show that Mondaquita Fault is a major structure with a wide associated damage zone. Within the damaged area, the proposed east-dipping thrust represents a back-thrust of the first order Mondaquita Fault, with ~500 m of vertical displacement (equivalent to the offset observed between age-elevation trends of each group of samples in the vertical profile). Other examples where faulted age-elevation profiles have been described in fold-and-thrust belt scenarios include the Pyrenees (Fitzgerald et al., 1999; Metcalf et al., 2009).

The number of confined track lengths (TL) measurements is unfortunately low (Nmax=18, see Table 1). However, these can still place some constrains on the thermal history of rocks in the absence of a more robust AFT data set. Except for the lowermost sample in the vertical profile (Hb-Th 01_18_90) for which a mean track length of 14.6 μm (N=1) was obtained, all samples presented a short mean track length (<14 µm) and tend toward bimodality, suggesting that samples did not experience a simple cooling history but had a more prolonged residence within a PAZ where shortening of tracks would occur (e.g., Gleadow et al., 1986).

The “breaks in slope” (upper/older and lower/younger) are not captured by our age/elevation data, thus we cannot constrain exactly when this PAZ was formed nor when it was exhumed. However, relative tectonic and thermal stability must have occurred from at least ~52 to 30 Ma that is the period of time of the obtained AFT ages. The cooling event that brought samples to surface must have occurred after the youngest AFT ages obtained for the samples (Hf_Th 01-18-90 and Hf_Th 01-18-110), i.e. after ~30 Ma. The earlier rapid cooling event, prior to the thermal stability that led to the development of the PAZ likely occurred prior to ca. 52 Ma, although our data does not constrain the exact time because the upper break in slope is not captured in the age-elevation profile. To constrain the timing of the two rapid cooling events, we rely on inverse thermal modeling.

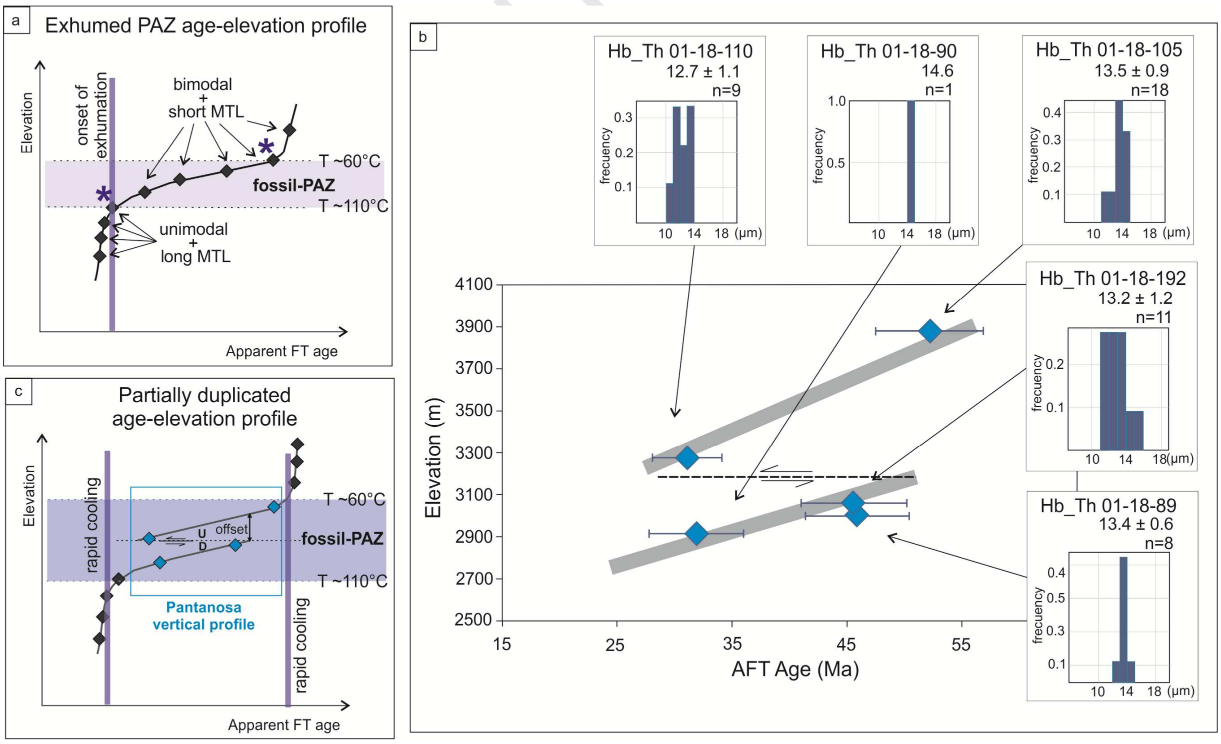

Figure 3: (a) Theoretical age-elevation profile showing an exhumed-PAZ for apatite (based on Fitzgerald et al., 1995). Breaks in slope are indicated by asterisks, and represents the paleo-isotherms that define the PAZ. The lower “convex-up” break in slope approximates the timing of onset of last episode of rapid cooling.. **(b) AFT** age-elevation profile from samples collected from the Pantanosa vertical transect at the Pantanosa River. Track length distributions

for each sample are shown, with mean track length and number of confined tracks measured. AFT ages error bars are 2σ. **(c)** Interpretation of age-elevation profile as being partially duplicated due to faulting. U=up and D=down refers to fault kinematic

4.2 Thermal modeling

Despite the relatively few number of confined tracks, the HeFTy inverse thermal modeling best-fit time-temperature paths (where goodness of fit is >0.95) for the four of the samples in the vertical transect show consistent results (Fig. 4). We do not model sample Hb_Th_01-18-90 because there is only one confined track measured. Models are characterized by an episode of rapid cooling at ~65-55 Ma, followed by a period of slow cooling (~1℃/Myr) between ~50 to ~15 Ma, and a final rapid cooling (~8-6℃/Myr) episode starting at ~15-10 Ma until present. Discrepancies between models are likely the result of the limited confined track measurements. HeFTy inverse thermal modelings are therefore consistent with our interpretation of the age-elevation profile as an exhumed PAZ, bracketed by rapid cooling episodes. A rapid cooling event starting at ca. 15-10 Ma is strongly supported by existing ~14 to 12 Ma AHe ages (Maydagán et al., 2020) from the same Pico Los Sapos Batholith, located <5 km west of our sampling area (Fig. 2).

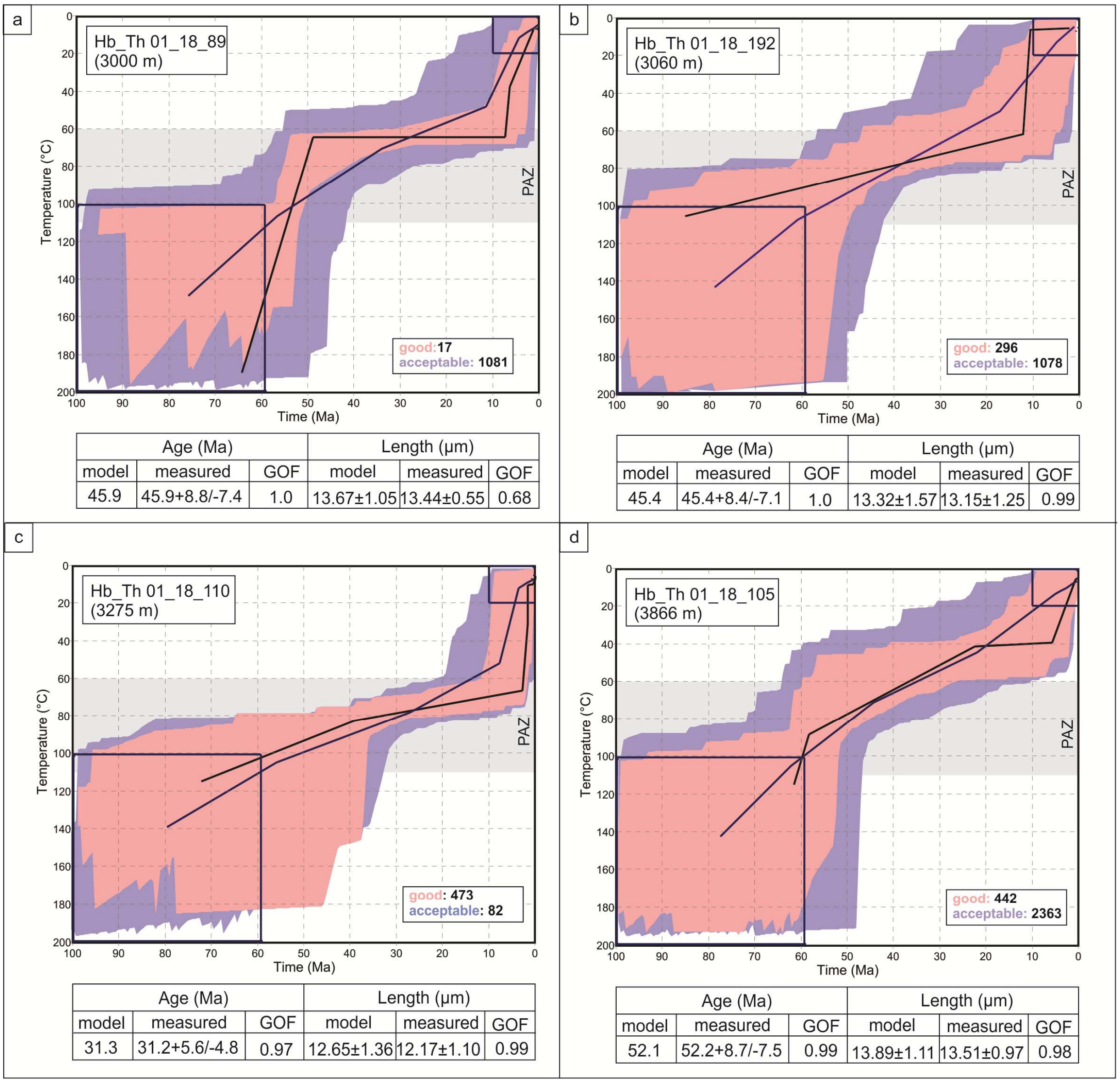

Figure 4: Thermal models obtained for the Pantanosa vertical transect samples produced using HeFTy (Ketcham, 2005). The pink envelope represents a good fit (i.e., the T-t paths that are supported by the data), and the light-colored blue envelope is an "acceptable fit" (T–t paths not ruled out by the data), for a duration of 20,000 random paths. The solid black line corresponds to the "best fit model" line and blue line represents an average path. Blue rectangles are the constraint boxes.

The thermochronological analyses performed in the High Andes at 31.5°S allows to place some constraints on the thermal evolution of the region. Summarizing, from the interpretation of the AFT age-elevation profile and the modeled t-T trajectories, together with previous AHe ages (Maydagán et al., 2020), we conclude that the thermal history of the region since Paleocene times includes rapid cooling at ~65-55 Ma, slow cooling and long-term residence of samples within a PAZ from ~52 to ~15 Ma, and a rapid cooling event starting at ca. 15-10 Ma. Samples from the vertical transect were collected in the hanging wall of the east-vergent Mondaquita reverse fault (Fig. 2), which juxtaposes the upper Paleozoic Pico Los Sapos Batholith and the Permo-Triassic Choiyoi Gr. over the volcaniclastic Oligo-Miocene Estratos de Mondaca unit. We interpret the overall observed thermal history to result from reverse faulting activity over this structure followed by erosion, which led to rapid cooling. During or following middle Miocene thrusting, back-thrusting juxtaposed the upper-two samples to higher levels in the age-elevation profile. The kinematic evolution of the proposed thermal history is shown in figure 5.

4.3 Kinematic and exhumation evolution

The integration of results from the thermochronological analysis and the kinematic modeling allow us to propose a three-stage model (Fig. 5). During the first stage, T1, which occurs between ~65 to 55 Ma, the samples are exhumed into the PAZ. Exhumation of the Carboniferous intrusive rocks via erosion of the Mesozoic deposits is achieved by movement along the Mondaquita Fault. On top of this unconformity, the lower Miocene sequences are deposited, including the Pachón Fm. lavas (23-21 Ma), the Estratos de Mondaca unit (22-21 Ma) and Neogene synorogenic deposits. During the second stage (T2), at ca. 15 Ma, the samples experienced rapid cooling as a result of vertical movement and exhumation of the Mondaquita hanging-wall, with an amount of exhumation >3 km. The final stage (T3) represents exposure of the samples after the final movement along the Mondaquita Fault, and associated backthrust, and the backtilting of its hanging-wall by movement along the Santa Cruz Fault located further east (Fig. 1 and Fig. 5).

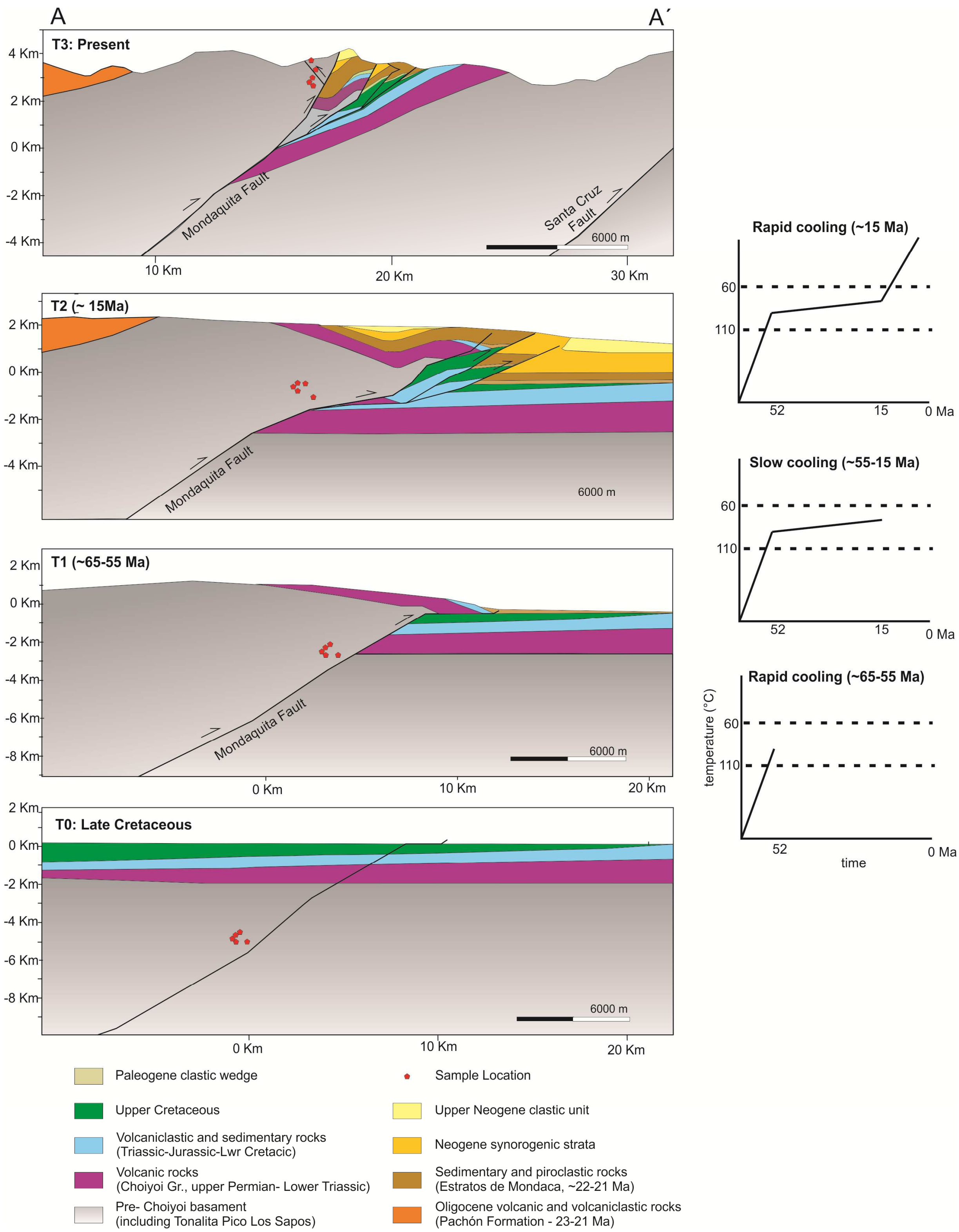

417

418 **Figure 5**: Structural and thermal evolution of the Cordón de Pantanosa area. Two episodes of rapid cooling are
419 recognized at ~65-55 Ma (T1) and at ~15 Ma (T2), separated by a period of tectonic quiescence and the

development of an apatite PAZ. The approximately position of the samples from the Pantanosa vertical profile is shown. Location of the cross section (A-A´) is shown in figure 2.

5. Discussion

Our data suggests that the core of the Andes mountains at 31.5°S, close to the water divider, was exhumed during two episodes of rapid cooling/exhumation. The first one occurred in the early Cenozoic (ca. 65-55 Ma) and the second one in the middle Miocene (beginning ca. 15-10 Ma), separated by a period of relative tectonic quiescence characterize by a slow cooling between ca. 52 Ma and ca. 15 Ma (Fig. 5). We interpret the observed thermal evolution as related to erosional cooling during and following tectonic activity along the Mondaquita reverse fault.

5.1 Early Cenozoic compressional phase

Late Cretaceous - early Cenozoic (~65 Ma) deformation grouped into the K-T tectonic phase is widely distributed in the Chilean Andes (Cornejo et al., 2003; Charrier et al., 2007; Martinez et al., 2017). In the western slope of the Andes, between 30° and 36°S, the uppermost Cretaceous volcaniclastic deposits of the Lo Valdés Formation (70 – 65 Ma) are interpreted to be associated to the late phase of an extensional period (Charrier et al., 2009). Immediately afterwards, a discrete event of Andean shortening has been ascribed to a period of rapid trench-perpendicular convergence velocity between the Nazca and South American plates (Pardo-Casas and Molnar, 1987; Sdrolias and Muller, 2006). Locally, the K-T contractional phase is evidenced by the unconformity between the Paleocene Estero Cenicero Fm. (Rivano and Sepúlveda, 1991; Mpodozis, 2015) and the underlying Cretaceous units, that crop up just west of our study area, in Chile. We correlate this event with the ~65-55 Ma compressional activity of the Mondaquita Fault. Although during this event, according to our proposed structural evolution (Fig. 5), erosion of the ~1.5 km Mesozoic sequences occurred, no contemporaneous synorogenic deposits are recognized locally. However, there are packages of sedimentary rocks in the intermountain deposits of Precordillera and within the Frontal Cordillera, that still lack for accurate age constraints and could potentially represent the unroofing sequences related to this early constructional orogenic pulse. For example, 65 Ma green mudstones and redbeds were identified by Reat and Fosdick (2018), in the easternmost Precordillera at Huaco, that could possibly represent the distal foredeep facies associated with early Cenozoic mountain building in the core of the Andes.

According to our interpretation of the Pantanosa AFT vertical profile, a period of relative quiescence and thermal stability since at least ~52 Ma to ~15 Ma allowed the formation of an apatite PAZ. Therefore, our data do not reflect episodes of rapid cooling during the late Eocene as evidenced in other sectors of the Andes to the north (Cembrano et al., 2003; Lossada et al., 2017; Rodríguez et al., 2018), indicating that early stages of Andean construction related to the Incaic orogenic phase (45-35 Ma, Steinmann, 1929) did not extend south of ~30°S.

5.2 Middle Miocene compression

Final exhumation of rocks at the Cordón de Pantanosa in the Frontal Cordillera occurred beginning ca. 15-10 Ma, as shown by our data, in support of Maydagán et al. (2020). Those authors presented the results from an apatite (U-Th)/He study performed in the Altar porphyry Cu (Au) deposit area, hosted in the Pachón Fm. (Fig. 2). They obtained two new AHe ages (3 grains per sample) of 14.3 ± 0.3 Ma and 11.87 ± 0.15 Ma from the same Carboniferous-Permian Pico Los Sapos Batholith we sampled, just ~8 km west of our vertical profile. Maydagán et al. (2020) further propose that the observed 11-10 Ma rapid cooling and related tectonic uplift in the Altar region, west of our sampling area (Fig. 2), was synchronous with the formation of hydrothermal systems, which had important implications increasing the Cu-Au grades of the deposits.

During the proposed middle Miocene rapid exhumation, rocks cooled at ~8-6°C/Myr, which transalets in an exhumation rate of ~240-320 m/Myr, assuming a paleo-geothermal gradient of ~25°C/km, typical of continental geotherms (Hamza & Muñoz, 1996; Morgan, 1984). At these rates advection of isotherms is not significant (e.g., Reiners and Brandon 2006) so this simple translation is valid. The presence of part of a fossil-PAZ exposed at high elevation indicates that exhumation during the ~15 Ma pulse exceeded >3 kms, allowing the denudation of rocks located below the 60°C paleo-isotherm (~2.4 km calculated for a geothermal gradient of 25°C/km). We interpret the AFT cooling ages as the result of fault slip along the Mondaquita Fault, with resultant erosion. South of our study area, the Mondaquita Fault thrusts the Pachón Fm. over the ca. 18 Ma Laguna del Pelado Volcanic Complex (Mpodozis et al., 2009; Mpodozis, 2016; Bergoing Rubilar, 2016) and the El Yunque Volcanic Unit (15–14 Ma; Mpodozis and

Cornejo, 2012), evidencing fault activity around 14 Ma as consistent with our interpretation. The Mondaquita Fault is the westernmost structure exhuming the Permo-Triassic volcanic rocks and granitoids of the Choiyoi Gr. (280-250 Ma, Sato et al., 2015), and uplifting the westernmost range of the Frontal Cordillera (i.e., the Cordón de Pantanosa, Fig. 1, Fig. 6). A detrital zircon U/Pb provenance study conducted in the adjacent synorogenic intermountain basins of Precordillera (Fig. 1) proposed that main uplift of the Frontal Cordillera ranges occurred between 17 to 14 Ma (Levina et al., 2014). However, the first contribution of a Permo-Triassic (248-280 Ma) source is recorded in the detrital signals from samples of ca. 14 Ma (in Pachaco and Talacasto localities, Fig. 1) to 8 Ma (Albarracín locality, Fig. 1). Given these results and the 14-12 Ma AHe dates (Maydagán et al., 2020) we believe it is most likely that exhumation related to erosion during Mondaquita fault activity took place at ca. 15 Ma, although our data suggest exhumation in the Cordón de Pantanosa at 15-10 Ma. Permo-Triassic volcanic provenance found in ca. 14 Ma foreland basin sediments correlates well with our proposal of an onset of rock uplift of the Choiyoi Gr. through the Mondaquita Fault at around 15 Ma.

Southeast of our study area, in the Manantiales Basin (32°S, Fig. 1, Fig. 6), recent geologic mapping, stratigraphic and structural studies, and integrated geochronologic and thermochronologic analyses were performed by Pinto et al. (2018), Mahoney et al. (2019), and Mackaman-Lofland et al. (2019), which allow to redefine the basin stratigraphy and place some constraints on the subsidence and exhumational patterns. Even though they propose different schemes, agree in the beginning of the sedimentation of the upper member in the early Miocene (~17 Ma). The onset of this Neogene subsidence in the Manantiales Basin is related with the eastward propagation of the La Ramada-FTB system and rock uplift of ranges in the Frontal Cordillera (Cordón de Pantanosa, Cordillera Santa Cruz, Cordón de Ansilta/Cordón del Espinacito, Fig. 1). Latitudinally, our study area correlates to the south with the external or easternmost sector of La Ramada-FTB (Cordón del Límite, Fig. 1, Fig. 6), as the Teatinos Fault is located at the same longitude but towards the south of the Mondaquita Fault. An onset of deformation at 17 Ma in the inner (western) sector of La Ramada-FTB (Pinto et al., 2018: Mahoney et al. 2019), is consistent with the middle to late Miocene exhumation event recorded in our data. Moreover, timing of fault activity of the innermost thrusts in La Ramada-FTB at ~32°S (Gonzáles, Totoral and Pelambres thrusts, Fig . 6) is constrained between 21 and 14 Ma, based on syn- and post-tectonic intrusive ages (Mpodozis, 2016).

The timing of deformation of the different morphostructural units at ~31.5°S is constrained by various studies. The Coastal Range deformation occurred during the Cretaceous, as indicated by AFT and AHe from Rodriguez et al. (2018). There are many ranges in the High Andes that still lack robust constraints on their uplift and exhumation history, especially those of Frontal Cordillera such us Cordillera Santa Cruz, Cordón de Ansilta and Cordón del Espinacito. For the domain located west and southwest of our sampling area, limited by the González, Totoral and Pelambres faults (Fig. 6), deformation is bracketed between 21 and 14 Ma (Mpodozis et al, 2009, 2016). To the southeast, the Cordillera del Tigre likely underwent uplift and exhumation at around 8 Ma, as shown by inversion of the Manantiales Basin recorded with AHe (Mahoney et al., 2019). The rise of the Precordillera constrained between ~12-9 Ma (Levina et al., 2014), suggests a foreland propagation of the deformation, after a first pulse of uplift in the Frontal Cordillera. Even though, our proposed 15-10 Ma rock uplift pulse in relation with Mondaquita Fault activity fills a sequence of deformation that becomes younger foreland-ward, during the last stage of Cenozoic deformation, more low-temperature thermochronological studies are needed in the Cordillera Santa Cruz and Cordón de Ansilta to fill the gaps of data regarding its onset of deformation.

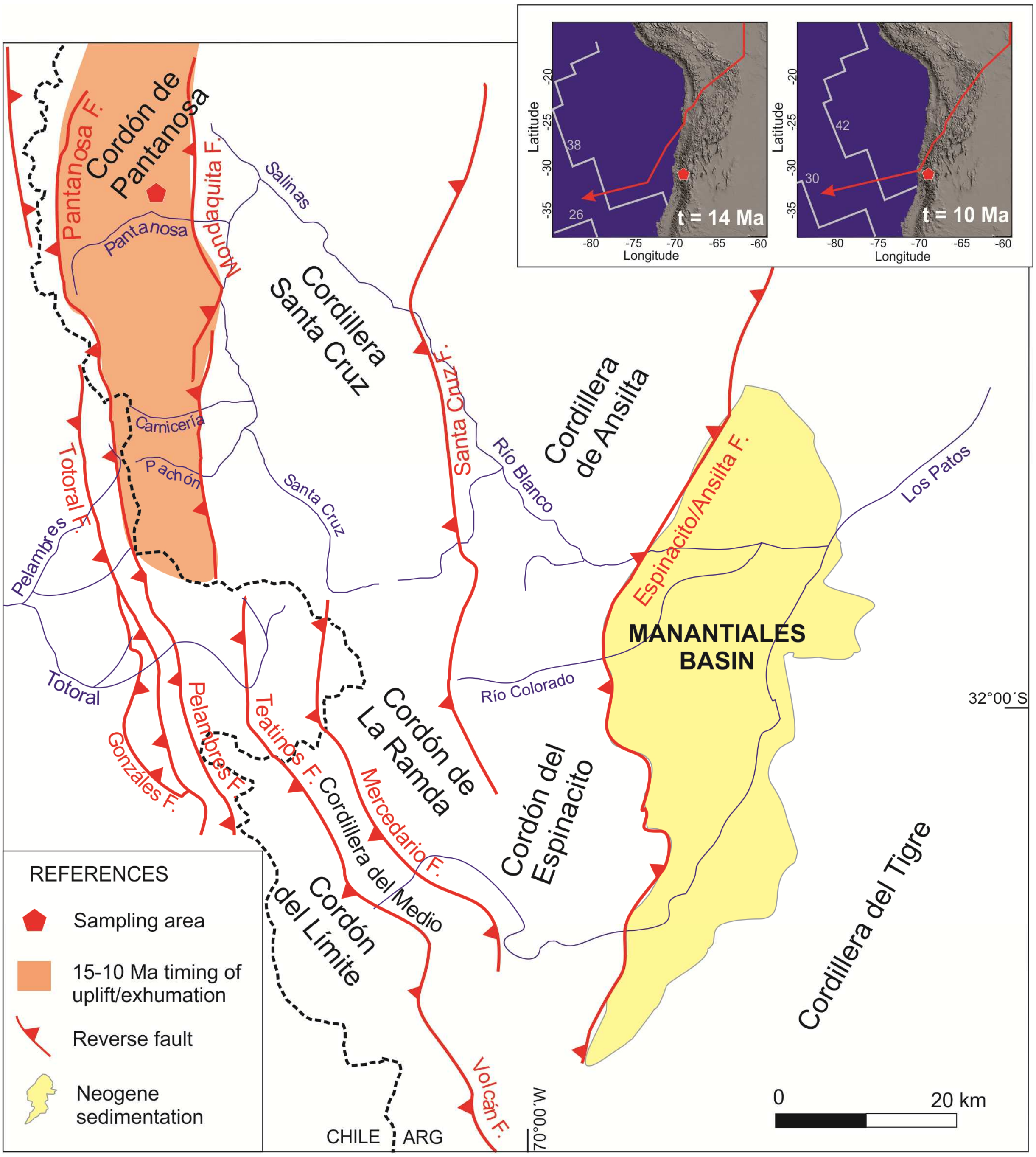

Figure 6: Regional context of the proposed ~15 Ma exhumation. Modified from Cristallini et al. (1994), Perez (2001) and Mpodozis (2016). Upper right panel shows the geodynamic context of Juan Fernández ridge (red arrows) collision against the South American margin at the time period of 12 to 14 Ma, after Yañez et al. (2002). At ca. 14 Ma, subduction point is located at ~25°S, faraway from our study area.

Considering the geodynamic scenario, the inference of a rising Frontal Cordillera previous to the flattening of the slab has been reported for other sectors of this mountain chain (Buelow et al., 2017; Fosdick et al., 2017; Lossada et al., 2017; 2020; Riesner et al., 2019). Taken within the context of the precision of our temporal constraints, the 15 Ma proposed exhumation of the core of the range at 31.5°S is clearly unrelated to the collision of the Juan Fernández aseismic ridge against this part of the South American continental margin at around 10 Ma, following Yañez et al.´s (2002) reconstructions (Fig. 6 upper-right pannel). Therefore, uplift of the Cordón de Pantanosais temporally decoupled from any increased mechanical coupling between plates during the flattening of the Nazca slab, as the effects of flattening at 31.5°S are evident since ca. 11-10 Ma (Maydagán et al., 2020), with the beginning of the collision of the W-E Juan Fernández ridge segment (Yañez et al., 2002; Fig. 6). Instead, we suggest that rock uplift of Cordón de Pantanosa in the Frontal Cordillera at ~31.5°S occurred in response to compressive stresses acting in the retroarc region during a "normal-type" subduction regime with a positive trench roll-back velocity (Uyeda, 1982; Martinod et al., 2010). A convergent retroarc system is likely the result of favorable trench normal convergence velocity and westward absolute motion of the overriding South American plate, orthogonal to the margin since the beginning of the Miocene (Maloney et al., 2013).

6. Conclusion

Together with other regional data, AFT analysis in the Cordón de Pantanosa, the westernmost range of the Frontal Cordillera, located in the core of the Andes at 31.5°S, unravels the thermal and exhumation history of this region. The recognition of parts of an exhumed-PAZ in the samples from a faulted vertical profile suggests that the region underwent a period of tectonic stability between >52 Ma and 20-15 Ma. The interpretation of the age-elevation profile together with the modeled T-t trajectories indicates two episodes of rapid cooling during the early Cenozoic (~65-55 Ma) and in the middle Miocene (beginning ca. 15 Ma). We interpret these rapid cooling episodes as related to erosion during discrete Andean constructional orogenic phases, through the tectonic activity of the Mondaquita Fault. This K-T compressional phase is also evidenced in the region by the regional unconformity between late Cretaceous and Paleogene units. The ~15 Ma phase of mountain building is supported by independent structural, geochemical and thermochronological constrains in the region and provenance evidence from the foreland basin system. An exhumation pulse beginning at ca. 15 Ma in the core of the mountain range indicates that horizontal shortening, thickening of the crust, and rock uplift/erosion most likely occurred prior to the collision at this latitude of the Juan Fernández aseismic ridge (ca. 10 Ma) and consequently prior to the establishment of the present day Pampean flat slab at 31.5°S. The proposed ca. 15 Ma contractional event in the core of the Andes completes a foreland-ward onset of uplift/exhumation sequence at 31.5°S starting with the Cretaceous deformation of the Coastal Range, the 21-14 Ma profound deformation in Principal Cordillera, the ca. 15 Ma proposed exhumation event in the westernmost Frontal Cordillera, middle to upper Miocene uplift of eastern basement blocks of Frontal Cordillera, migration of the deformation front to Precordillera in the upper Miocene and foreland fragmentation in the Pliocene. Finally, our data do not reflect episodes of rapid cooling during the late Eocene as evidenced in other sectors of the core of the Andes north of 30°S, suggesting that the Incaic orogenic phase did not extend south of ~30°S, or it was restricted to the Coastal Range domain.

Acknowledgments

This work was supported by CONICET (PICT 2016-0269) and SEGEMAR.

References

Alarcón, P., and Pinto, L. 2015. Neogene erosion of the Andean Cordillera in the flat-slab segment as indicated by petrography and whole-rock geochemistry from the Manantiales Foreland Basin (32–32 30′ S). Tectonophysics, 639, 1-22.

Allmendinger, R.W. (2001), FaultKinWinFull versión 1.2.2. A program for analyzing fault slip data for WindowsTM computers.http://www.geo.cornell.edu/geology/faculty/RWA/programs.html

Allmendinger, R. W., and Judge, P. A. 2014. The Argentine Precordillera: A foreland thrust belt proximal to the subducted plate. Geosphere, 10(6), 1203-1218.

Allmendinger, R.W., D., Figueroa, D. Snyder, C. Beer, C. Mpodozis, Isacks, B. L. 1990. Foreland shortening and crustal balancing in the Andes at 30°S latitude, Tectonics, 9, 789-809.

Álvarez, P.P., 1996. Los Depósitos Triásicos y Jurásicos de la Alta Cordillera de San Juan. In: Ramos, et al. (Eds.), Geología de la Región del Aconcagua, Provincias de San Juan y Mendoza, Anales, vol. 24(5). Subsecretaría de Minería de la Nación, Dirección del Servicio Geológico, Buenos Aires, p. 59-137.

Álvarez, P.P., Ramos, V.A. 1999. The Mercedario rift system in the principal Cordillera of Argentina and Chile (32ºS). Journal of South American Earth Sciences 12, p. 17-31.

Bergoeing Rubilar, J. P. 2016. Evolución geoquímica del magmatismo de la Región de Los Pelambres (31°S) entre el cretácico superior y el mioceno superior: implicancias para la evolución tectónica y metalogénica de los Andes de Chile Central, Universidad de Chile, Degree thesis, 137p

Braun, J.; 2002. Quantifying the effect of recent relief changes on age–elevation relationships. Earth Planet. Sci. Lett. 200 (3–4), 331–343.

Buelow, E.K., Suriano, J., Mahoney, J.B., Kimbrough, D.L., Mescua, J.F., Giambiagi, L., Hoke, G.D., 2018. Sedimentologic and stratigraphic evolution of the Cacheuta basin: Constraints on the development of the Miocene retroarc foreland basin, south-Central Andes. Lithosphere: 1:26. doi.org/10.1130/L709.1.

Cahill, T. and Isacks, B. L., 1992. Seismicity and shape of the subducted Nazca plate. Journal of Geophysical Research 97: 17503-17529.

Cembrano, J., M. Zentilli, A. Grist and G .Yáñez, 2003. Nuevas edades de trazas de fisión para Chile Central (30-34°S): Implicancias en el alzamie nto y exhumación en los Andes desde el Cretácico. X Congr. Geol. Chileno, Universidad de Concepción, Concepción, Chile.

Cristallini, E.O., Ramos, VA. 2000. Thick-skinned and thin-skinned thrusting in La Ramada fold and thrust belt: Crustal evolution of the High Andes of San Juan, Argentina (32°SL). Tectonophysics 317: p. 205-235.

Cristallini, E., Mosquera, A., Ramos, V.A., 1994. Estructura de la Alta Cordillera de San Juan. Revista de la Asociación Geológica Argentina 49 (1-2), p. 165-183.

Fitzgerald, P. G., and Gleadow, A. J., 1990. New approaches in fission track geochronology as a tectonic tool: Examples from the Transantarctic Mountains. International Journal of Radiation Applications and Instrumentation. Part D. Nuclear Tracks and Radiation Measurements, 17(3), 351-357.

Fitzgerald, P.G., R.B. Sorkhabi, T.F. Redfield, Stump E. 1995. Uplift and denudation of the central Alaska Range: A case study in the use of apatite fission track thermochronology to determine absolute uplift parameters. Journal of Geophysical Research, 20: 175-191.

Gans C.R., Beck S.L., Zandt G., Gilbert H., Alvarado P., Anderson M., Linkimer L. 2011. Continental and oceanic crustal structure of the Pampean flat slab region, western Argentina, using receiver function analysis: new high resolution results. Geophys. J. Int.; 186(1):45-58.

Gleadow, A. J. W.,1981. Fission-track dating methods: what are the real alternatives?. Nuclear Tracks, 5(1-2), 3-14.

Gleadow, A. J. W., and Duddy, I. R., 1981. A natural long-term track annealing experiment for apatite. Nuclear Tracks, 5(1-2), 169-174.

Gleadow, A. J. W., & Fitzgerald, P. G., 1987. Uplift history and structure of the Transantarctic Mountains: new evidence from fission track dating of basement apatites in the Dry Valleys area, southern Victoria Land. Earth and planetary science letters, 82(1), 1-14.

Gleadow, A. J. W., Duddy, A. I., and Lovering, J. F., 1983. Fission track analysis: a new tool for the evaluation of thermal histories and hydrocarbon potential. The APPEA Journal, 23(1), 93-102.

Gleadow AJW, Duddy IR, Green PF, Lovering JF, 1986. Confined fission track lengths in apatite: a diagnostic tool for thermal history analysis. Contrib Mineral Petrol 94:405–415

Green, P. F., Duddy, I. R., Laslett, G. M., Hegarty, K. A., Gleadow, A. W., and Lovering, J. F., 1989. Thermal annealing of fission tracks in apatite 4. Quantitative modelling techniques and extension to geological timescales. Chemical Geology: Isotope Geoscience Section, 79(2), 155-182.

Hamza, V. M., and Muñoz, M., 1996. Heat flow map of South America. Geothermics, 25(6), 599-646.

Heredia, N., Fernández, L. R., Gallastegui, G., Busquets, P., and Colombo, F., 2002. Geological setting of the Argentine Frontal Cordillera in the flat-slab segment (30°00′–31°30′ S latitude). Journal of South American Earth Sciences, 15(1), 79-99.

Huntington, K. W., T. A. Ehlers, K. V. Hodges, and D. M. Whipp Jr., 2007. Topography, exhumation pathway, age uncertainties, and the interpretation of thermochronometer data, Tectonics, 26, TC4012, doi:10.1029/2007TC002108.

Hurford, A.J., and Green, P.F., 1982, A users' guide to fission track dating calibration: Earth and Planetary Science Letters, v. 59, p. 343-354.

Hurford, A.J., and Green, P.F, 1983, The zeta age calibration of fission-track dating: Chemical Geology, v. 41, p. 285-317.

Jordan, T. E., Isacks, B. L., Allmendinger, R. W., Brewer, J. A., Ramos, V. A., Ando, C. J. 1983. Andean tectonics related to geometry of subducted Nazca plate. Geological Society of America Bulletin, 94(3), 341-361.

Jordan T. E., Tamm V., Figueroa G., Flemings P. B., Richards D., Tabbutt K., Cheatham T. 1996. Development of the Miocene Manantiales foreland basin, Principal Cordillera, San Juan, Argentina. Andean Geol 23(1): 43-79.

Ketcham, R.A., 2005. Forward and inverse modeling of low-temperature thermochronometry data. In: Reiners PW, Ehlers TA (eds) Low-temperature thermochronology: techniques, interpretations, and applications. Reviews in Mineralogy and Geochemistry, Mineralogical Society of America 58, pp 275–314

Ketcham RA, A. Carter, R.A. Donelick, J. Barbarand and A.J. Hurford, 2007a. Improved modeling of fission-track annealing in apatite. Am Mineral 92:799–810

Ketcham, R.A., A. Carter, R.A. Donelick, J. Barbarand, and A.J. Hurford, 2007b. Improved measurement of fission-track annealing in apatite using c-axis projection. Am Mineral 92:789–798

Kay, S. M., and Mpodozis, C. 2002. Magmatism as a probe to the Neogene shallowing of the Nazca plate beneath the modern Chilean flat-slab. Journal of South American Earth Sciences, 15(1), 39-57.

Levina, M., Horton, B. K., Fuentes, F., Stockli, D. F. 2014. Cenozoic sedimentation and exhumation of the foreland basin system preserved in the Precordillera thrust belt (31-32°S), southern central Andes, Argentina. Tectonics, 33(9), 1659-1680. https://doi.org/10.1002/2013TC003424

Llambías, E. J., and Sato, A. M. 1990. El batolito de Colangüil (29°- 31°S), Cordillera Frontal de Argentina: estructura y marco tectónico. Revista Geológica de Chile 17(1): p. 99-108. Santiago.

Löbens, S., E. R. Sobel, F. A. Bense, K. Wemmer, I. Dunkl, and S. Siegesmund. 2013. Refined exhumation history of the northern Sierras Pampeanas, Argentina, Tectonics, 32, 453–472, doi:10.1002/tect.20038.

Lossada, A. 2018. Estudio de la exhumación y levantamiento cenozoico de la Cordillera Frontal, entre los 30°y 34.8°S, Andes Centrales Sur. PhD T hesis, Universidad de Buenos Aires, 208pp.

Lossada, A., Giambiagi, L., Hoke, G., Fitzgerald, P., Creixell, Ch., Murillo, I., Mardonez, D., Velásquez, R, Suriano, J., 2017. Thermochronologic evidence for late Eocene Andean mountain building at 30°S. Tectonics 36, doi.org/10 .1002/2017TC004674

Lossada, A., Hoke, G., Giambiagi, L., Fitzgerald, P., Mescua, J., Suriano J., Aguilar A., 2020. Detrital thermochronology reveals major middle Miocene exhumation of the eastern flank of the Andes that predates the Pampean flat-slab (33º-33.5ºS). *Tectonics*, *39*(4), e2019TC005764.

Maloney, K. T., Clarke, G. L., Klepeis, K. A., & Quevedo, L., 2013. The Late Jurassic to present evolution of the Andean margin: Drivers and the geological record. Tectonics, 32(5), 1049-1065.

Marot, M., Monfret, T., Gerbault, M., Nolet, G., Ranalli, G., Pardo, M. 2014. Flat versus normal subduction zones: a comparison based on 3-D regional traveltime tomography and petrological modelling of central Chile and western Argentina (29°–35°S). Geophysical Journal International, 199(3), p. 16.

Maydagán, L., Zattin, M., Mpodozis, C., Selby, D., Franchini, M., & Dimieri, L., 2020. Apatite (U–Th)/He thermochronology and Re–Os ages in the Altar region, Central Andes (31°30′S), Main Cordillera of San Juan, Argentina: implications of rapid exhumation in the porphyry Cu (Au) metal endowment and regional tectonics. Mineralium Deposita, 1-20.

Maydagán L. 2012. El Prospecto de Cu–(Au–Mo) Altar (31°29′LS, 70°28′LO), San Juan: Unpublished PhD thesis, Bahía Blanca, Argentina, Universidad Nacional del Sur, 340 p

Maydagán L, Franchini M, Chiaradia M, Pons J, Impiccini A, Toohey J, Rey R, 2011. Petrology of the Miocene igneous rocks in the Altar region,main Cordillera of San Juan,Argentina. A geodynamic model within the context of the Andean flat-slab segment and metallogenesis. J S Am Earth Sci 32(1):30–48

Maydagán L, Franchini M, ChiaradiaM, Dilles J, Rey R, 2014. The altar porphyry Cu–(Au–Mo) deposit (Argentina): a complex magmatichydrothermal system with evidence of recharge processes. Econ Geol 109(3):621–641.

Mahoney, B.; Mazzitelli, M.; Suriano, J.; Kimbrough, D., Metcalf, J.; Lossada, A.; Giambiagi, L.; Mescua, J., 2019. Evolution of the Miocene Manantiales Basin, South-Central Andes: Evidence for Strongly Coupled Rapid Basin Subsidence and Exhumation AAPG ACE 2019 - Annual Conference and Exhibition. San Antonio.

Malusà, M. G., & Fitzgerald, P. G. 2019. Application of thermochronology to geologic problems: Approaches and conceptual models. In M. G. Malusà, & P. G. Fitzgerald (Eds.), Fission track thermochronology and its application to geology (pp. 191–209). Cham: Springer. https://doi.org/10.1007/978-3-319-89421-8_10

Martinod, J., Husson, L., Roperch, P., Guillaume, B., & Espurt, N., 2010. Horizontal subduction zones, convergence velocity and the building of the Andes. Earth and Planetary Science Letters, 299(3-4), 299-309.

Martinod, J., Guillaume, B., Espurt, N., Faccenna, C., Funiciello, F., & Regard, V., 2013. Effect of aseismic ridge subduction on slab geometry and overriding plate deformation: Insights from analogue modeling. Tectonophysics, 588, 39-55.

Metcalf, J. R., Fitzgerald, P. G., Baldwin, S. L., & Muñoz, J. A.,2009. Thermochronology of a convergent orogen: Constraints on the timing of thrust faulting and subsequent exhumation of the Maladeta Pluton in the Central Pyrenean Axial Zone. Earth and Planetary Science Letters, 287(3-4), 488-503.

Mirré, J., 1966. Geología del valle del Río de Los Patos (entre Barreal y Las Hornillas). Revista de La Asociación Geológica Argentina, 21(4), 211–231.

Morgan, P., 1984. The thermal structure and thermal evolution of the continental lithosphere. Physics and Chemistry of the Earth, 15, 107–193

Mpodozis, C. 2016. Mapa Geológico Regional del Área de Los Pelambres (esc 1:75.0000). Informe Interno, Antofagasta Minerals, Santiago.

Mpodozis, C., and Kay, S. M. 1990. Provincias magmáticas ácidas y evolución tectónica de Gondwana: Andes chilenos (28-31 S). Andean Geology, 17(2), 153-180.

Mpodozis, C. and Ramos, V.A. 1989. The Andes of Chile and Argentina. In Ericksen, G.E., M.T. Cañas Pinochet y J.A. Reinemud (eds.) Geology of the Andes and its relation to Hydrocarbon and Mineral Resources, Circumpacific Council for Energy and Mineral Resources, Earth Sciences Series 11: p. 59-90, Houston.

Mpodozis, C., Rivano, S., Parada, M.A., Vicente, J.C. 1976. Acerca del plutonismo tardi-hercínico en la Cordillera Frontal entre los 30-33°S (Provincias de San Juan y Mendoza, Argentina, Coquimbo, Chile). In Congreso Geológico Argentino, No. 6, Actas, p. 143-171. Bahía Blanca.33-1654.

Mpodozis, C., Brockway, H.; Marquardt, C; Perelló, J. 2009. Geocronología U/Pb y tectónica de la región de Los Pelambres-Cerro Mercedario: implicancias para la evolución cenozoica de Los Andes del centro de Chile y Argentina. In Congreso Geológico Chileno, No.12., Santiago.

Musso, R. J. E., Pérez, D. J., Rey, R., Toohey, J. 2012. Geología de las nacientes del río La Pantanosa, Cordillera Frontal (31 33'S), Provincia de San Juan, Argentina. In: XIII Congreso Geológico Chileno. Antofagasta pp 250–251

Oliveros, V., Féraud, G., Aguirre, L., Fornari, M.; Morata, D. 2006. The Early Andean Magmatic Province (EAMP): 40Ar/39Ar dating on Mesozoic volcanic and plutonic rocks from the Coastal Cordillera, Northern Chile. Journal of Volcanology and Geothermal Research 157: 311-330

Ortiz, G., Alvarado, P., Fosdick, J. C., Perucca, L., Saez, M., & Venerdini, A., 2015. Active deformation in the northern sierra de Valle Fértil, sierras Pampeanas, Argentina. Journal of South American Earth Sciences, 64, 339-350.

Perelló J, Sillitoe RH, Mpodozis C, Brockway H, Posso H., 2012. Geologic setting and evolution of the porphyry copper–molybdenum and copper–gold deposits at Los Pelambres, Central Chile. Soc Econ Geol Spec Pub 16:79–104

Pérez D. J., 1995. Estudio geológico del cordón del Espinacito y regiones adyacentes, provincia de San Juan. (unpublished) PhD Thesis, Universidad de Buenos Aires

Pérez D. J., 2001. Tectonic sand unroofing history of Neogene Manatiales foreland basin deposits, Cordillera Frontal (32°30´S), San Juan pr ovince, Argentina. J South Am Earth Sci 14: 693-705

Pinto, L., Alarcón, P., Morton, A., Naipauer, M., 2018. Geochemistry of heavy minerals and U–Pb detrital zircon geochronology in the Manantiales Basin: Implications for Frontal Cordillera uplift and foreland basin connectivity in the Andes of central Argentina. Palaeogeography, Palaeoclimatology, Palaeoecology, 492, 104-125. https://doi.org/10.1016/j.palaeo.2017.12.017

Ramos, V. A., and Folguera, A., 2009. Andean flat-slab subduction through time. Geological Society, London, Special Publications, 327(1), 31-54.

Ramos, V.A.; Cegarra, M.; Cristallini, E., 1996. Cenozoic tectonics of the High Andes of west-central Argentina (30-36°S latitude). Tectonophysic s 259: p. 185-200.

Ramos, V.A., Cristallini, E., Pérez, D., 2002. The Pampean flat slab of the Central Andes: Journal of South American Earth Sciences, v. 15, p. 59–78.

Riesner, M., Simoes, M., Carrizo, D., and Lacassin, R., 2019. Early exhumation of the Frontal Cordillera (Southern Central Andes) and implications for Andean mountain-building at~ 33.5°S. Scientific reports, 9(1), 1-10.

Rivano, S., and Sepúlveda, P., 1991. Hoja Illapel. Servicio Nacional de Geología y Minería. Carta Geológica de Chile, 69(1), 250-00.

Rodríguez MP, Charrier R, Brichau S, Carretier S, Farías M, de Parseval P, Ketcham R.A. 2018. Latitudinal and longitudinal patterns of ex-humation in the Andes of North-Central Chile. Tectonics 37(9): 2863–2886.

Sato, A. M., and Llambías, E. J., 1993. El grupo Choiyoi, provincia de San Juan: equivalente efusivo del batolito de Colangüil. In Congreso Geológico Argentino (No. 12, pp. 156-165).

Sato, A. M., Llambías, E. J., Basei, M. A., and Castro, C. E., 2015. Three stages in the Late Paleozoic to Triassic magmatism of southwestern Gondwana, and the relationships with the volcanogenic events in coeval basins. Journal of South American Earth Sciences, 63, 48-69.

Steinmann, G., 1929. Geologie von Peru: Heidelberg, Germany, Karl Winter, 448 p

Suriano, J., Mardonez, D., Mahoney, J. B., Mescua, J. F., Giambiagi. L. B., Kimbrough, Lossada, A., 2017. Uplift sequence of the Andes at 30°S: insights from sedimentology and U/Pb dating of synorogenic deposits. Journal of South American Earth Sciences 75: (11–34)

Uyeda, S., 1982. Subduction zones: an introduction to comparative subductology. Tectonophysics 81, 133–159

Wagner, G. A., & Reimer, G. M., 1972. Fission track tectonics: the tectonic interpretation of fission track apatite ages. Earth and Planetary Science Letters, 14(2), 263-268.

Yáñez, G., Cembrano, J., Pardo, M., Ranero, C., and Selles, D., 2002. The Challenger–Juan Fernández–Maipo major tectonic transition of the Nazca–Andean subduction system at 33–34 S: geodynamic evidence and implications. Journal of South American Earth Sciences, 15(1), 23-38.

Sample	**Location** **Lat./Long.**	**Elev.** **(m)**	**N**	**Rho D** **(x10^6 cm^{-2})** **(Nd)**	**Rho-S** **(x10^5 cm^{-2})** **(Ns)**	**Rho-I** **(x10^6 cm^{-2})** **(Ni)**	**Age disp.** **(%)**	**P(χ^2)** **(%)**	**Central Age ±1σ** **(Ma)**	**[U]** **(ppm)**	**Confined track (mean length ± S.E., (N); µm)**	**Dpar (mean ± S.D.; µm)**
Hb_Th 01-18-90	31.535 °S 70.365 °W	2915	33	7.01 (5000)	1.65 (164)	6.54 (650)	0.24	17.96	**31.9 ± 4.1**	13.99	**14.6** **(1)**	1.4 ± 0.1
Hb_Th 01-18-89	31.535 °S 70.382 °W	3000	35	7.11 (5000)	2.62 (453)	7.25 (1251)	0.03	71.87	**45.9 ± 4.5**	14.52	**13.4 ± 0.6** **(8)**	1.4 ± 0.3
Hb_Th 01-18-192	31.540 °S 70.361 °W	3060	35	6.69 (5000)	3.24 (533)	8.52 (1402)	0.16	17	**45.6 ± 4.6**	19.18	**13.2 ± 1.2** **(11)**	1.5 ± 0.1
Hb_Th 01-18-110	31.545 °S 70.363 °W	3275	29	6.8 (5000)	9.53 (571)	37.08 (2223)	0.09	19.66	**31.3 ± 3.0**	78.91	**12.7 ± 1.1** **(9)**	1.4 ± 0.1
Hb_Th 01-18-105	31.503 °S 70.348 °W	3866	35	6.9 (5000)	7.13 (1082)	16.82 (2551)	0.03	53.96	**52.2 ± 4.7**	35.74	**13.5 ± 0.9** **(18)**	1.4 ± 0.2

- Cenozoic exhumation in the core of the Andes (31.5°S) reveal by AFT thermochronology
- two episodes of rapid cooling during the early Cenozoic and the middle Miocene
- Tectonic quiescence and relative thermal stability between ~55 to 15 Ma

Declaration of interests

☒ The authors declare that they have no known competing financial interests or personal relationships that could have appeared to influence the work reported in this paper.

☐The authors declare the following financial interests/personal relationships which may be considered as potential competing interests: